Published in final edited form as:
Langmuir. 2007 February 27; 23(5): 2655–2662. doi:10.1021/la062163s.

Layer-by-layer films from hyaluronan and amine modified hyaluronan

Aurore Schneider[1,3], **Catherine Picart**[1,5], **Bernard Senger**[1,2], **Pierre Schaaf**[4], **Jean-Claude Voegel**[1,2], and **Benoit Frisch**[3]

1*Institut National de la Santé et de la Recherche Médicale, INSERM Unité 595, 11 rue Humann, 67085, Strasbourg Cedex, France*

2*Faculté de Chirurgie Dentaire, Université Louis Pasteur, 1 place de l'Hôpital, 67000 Strasbourg, France*

3*Laboratoire de Chimie Enzymatique et Vectorisation LC01, UMR 7175 CNRS-Université Louis Pasteur, 74 route du Rhin, 67 400 Illkirch, France*

4*Institut Charles Sadron, Centre National de la Recherche Scientifique, Université Louis Pasteur, 6 rue Boussingault, 67083 Strasbourg Cedex, France*

5*Université de Montpellier 2, CNRS UMR 5539, Place Eugène Bataillon, 34095 Montpellier Cedex 5*

Abstract

Hyaluronan is a polysaccharide that is increasingly investigated for its role in cellular adhesion and for the preparation of biomimetic matrices for tissue engineering. Hyaluronan gels are prepared for application as space fillers whereas hyaluronan films are usually obtained by adsorbing or grafting a single hyaluronan layer onto a biomaterial surface. Here, we examine the possibility to employ the layer-by-layer technique to deposit thin films of cationic modified hyaluronan (HA^+) and hyaluronan (HA) of controlled thicknesses. The buildup conditions are investigated and growth is compared to that of other polyelectrolyte multilayer films containing either HA as polyanion or HA^+ as polycation. The films could be formed in a low ionic strength medium but required to be cross-linked prior to be put in contact with physiological medium. NIH3T3 fibroblasts were perfectly viable on self-assembled hyaluronan films with however a preference for hyaluronan ending films. These findings point out the possibility to tune the thickness of thin hyaluronan films at the nanometer scale. Such architectures could be employed for investigating cell/substrate interactions or for functionalizing biomaterial surfaces.

INTRODUCTION

Hyaluronan is a linear polysaccharide constituted of alternated N-acetyl-β-D-glucosamine and β -D- glucuronic acid residues, which is currently widely and increasingly investigated for its properties in biomedical applications [1,2,3,4]. Hyaluronan has not only peculiar physical properties in terms of hydration, viscosity and hydrogel formation but it becomes more and more investigated for its specific biological and bioactive properties and its implications in cell adhesion properties [5,6] and motility [7]. One of the main applications of hyaluronan concerns tissue engineering, where it has been mostly used to form a wide variety of hydrogels [8–10]. Several strategies have been developed to prepare these gels and rely usually on the introduction of chemically modified groups or on its complexation with cationic biopolymers (such as chitosan or collagen at acidic pHs) such as to form composite hydrogels [11,12]. Different types

Correspondence to: Catherine Picart, catherine.picart@univ-montp2.fr.

of cross-linkable and biodegradable hydrogels have thus been prepared based on various coupling chemistries performed either on carboxylic or on alcohol groups [8,13 10]. Photo-cross-linkable hyaluronan based on methacrylate hyaluronan conjugates have also been prepared [14, 15]. A great amount of work was also devoted to its chemical modification in order to prepare functional groups for the subsequent introduction of drugs into the hydrogels [16 17]. Another application of hyaluronan is to prepare a hyaluronan thin layer by direct and passive adsorption of hyaluronan solutions onto surfaces [18] or by covalently grafting hyaluronan onto surfaces [19]. The layer-by-layer technique, which was introduced approximately ten years ago by Decher and coworkers [20–22] is particularly suited for building thin films with a thickness control at the nanometer scale. It is also increasingly used in the biomedical field [23 24 25 26] and several types of natural polyelectrolytes, proteins, peptides, or viruses have been introduced in the films [27]. Recently, hyaluronan was also introduced in layer-by-layer assemblies in combination with different polycations and biopolymers such as poly(L-lysine) (PLL) [28 29], chitosan (CHI) [30,31], polyallylamine hydrochloride (PAH) [32] and collagen (COLL) [33,34]. (CHI/HA) and (PLL/HA) film growth in physiological medium was found to be of exponential type whereas (COLL/HA) films, which had to be assembled in a low ionic strength medium, exhibited a linear increase of the thickness as a function of the number of layers [33,34]. However, at present, there is no possibility to build thin films constituted only of hyaluronan and that have a controlled thickness at the nanometer scale.

The present work is aimed at evaluating the possibility to build molecular assemblies composed only of hyaluronan. Toward this end, an amine modified hyaluronic acid was prepared (which will be noted here cationic hyaluronic acid HA^+) and assembled with the unmodified anionic hyaluronan using the layer-by-layer technique. In this study, we will mainly focus on the buildup process and on the physico-chemical characteristics of the films. We will also evaluate the biocompatibility of this new kind of films.

EXPERIMENTAL

Synthesis of HA^+

N-(3-dimethylaminopropyl)-N'-ethylcarbodiimide (EDC) was purchased from Sigma-Aldrich; Sodium N-Hydroxysulfosuccinimide (Sulfo-NHS) was obtained from Accross and N-ethyl diisopropylamine (DIPA) from Alfa Aesar. The monoprotected di-amine (NH_2-Peg_2-NHBoc) is commercially available from Iris Biotech Marktredwitz (Germany). The aqueous solution of HA sodium salt (100 mg, 15 mmol) was dialyzed against 0.01N HCl (1.5 L) for 20h and then against water (miliQ grade) (1.5 L) for an additional 20h to convert the sodium salt to the acid form. The acid form of HA was recovered by lyophilization to give 76 mg of product.

100 mg (0.26 mmol of acid group) of acidic form of HA, 46 mg (0.39 mmol) of N-hydroxysulfosuccinimide (Sulfo-NHS) were dissolved in 8 mL of dry DMSO. 76 mg of 1-ethyl-3-(3-dimethylamino-propyl)carbodiimide (EDC) (0.39 mmol) were dissolved in the mixture under stirring. The reaction was allowed to proceed for 30 min. at room temperature. Then the amine (NH_2-Peg_2-NHBoc) (131 mg, 0.53 mmol, 2 eq) and DIPA (41 mg, 0.32 mmol, 1.2 eq) were added under stirring. The reaction was allowed to proceed for 4 days. After this time, the whole reaction mixture was poured into acetone (80 mL) to precipitate the resulting HA-protected amine. The solid was washed with acetone (3 × 80 mL), and then dried under vacuum to give 102 mg of crude product. 15 mg of HA-protected amine was dissolved in trifluoroacetic acid (TFA, 1.5 ml) at 0°C and stirred for 20 h at 4°C. 6 mL of water at 0°C were added to this mixture and the solution was neutralised with NaOH. The mixture was dialyzed against 0.1 M NaCl (1.5 L) for 20h and then against water miliQ (1.5 L) for an additional 20h. The product was recovered by lyophilisation. The degree of substitution was calculated by

integration of the methyl of acetamido moiety of GlcNAc residues resonance (δ = 2.05 ppm, 3H) relative to the methylene group near the primary amine (δ = 2.93 ppm, 2H).

Polyelectrolyte solutions

Anionic hyaluronan solutions (HA, 400 kDa, Bioiberica, Spain), poly(L-glutamic acid) (Sigma, P4886, M_w=60 000 g/mol), poly(L-lysine, Sigma, 60 000 g/mol), and poly(allylamine) hydrochloride (Aldrich, 283223, M_w=70 000) were prepared by dissolution at 0.5 mg/mL in a 0.01 M or 0.15 M NaCl aqueous solution at pH 6.5. Poly(ethylene imine) (Sigma, P3143, M_w≈750 000) was dissolved at 2 mg/mL in the same aqueous solution than that used for the buildup. It was always deposited as first layer. During film construction, all the rinsing steps were performed in the same aqueous solution at pH 6.5.

Films characterization by quartz crystal microbalance with dissipation monitoring (QCM-D) and atomic force microscopy (AFM)

The PEI-$(HA/HA^+)_i$ film buildup (where *i* denotes the number of layer pairs) was followed by *in situ* quartz crystal microbalance (QCM-Dissipation, Qsense, Sweden) [35,36]. The quartz crystal was excited at its fundamental frequency (about 5 MHz, ν = 1) as well as at the third, fifth and seventh overtones (ν = 3, 5 and 7 corresponding to 15, 25 and 35 MHz, respectively). Changes in the resonance frequencies Δ*f* and in the relaxation of the vibration once the excitation is stopped were measured at the four frequencies. Other films were also investigated in the same experimental conditions: PEI-$(PGA/HA^+)_i$, PEI-$(HA/PLL)_i$ and PEI-$(HA/PAH)_i$. For more clarity, the PEI precursor layer will be omitted in the subsequent notations.

The films were also imaged in contact mode in liquid with the Nanoscope IV from Veeco (Santa Barbara, CA) [37]. Deflection and height mode images were scanned simultaneously at a fixed scan rate (2 Hz) with a resolution of 512×512 pixels. The mean roughness of the films was measured over 5μm×5μm areas. It was calculated according to:

$$R=\frac{1}{N_x N_y}\sum_{i=1}^{N_x}\sum_{j=1}^{N_y}|z_{ij}-z_{\text{mean}}|$$ where z_{ij} is the height of a given pixel, z_{mean} is the average height of the pixels, and N_x and N_y are the number of pixels in the x and y directions.

Film characterization and cross-linking by FTIR

For the chemical cross-linking of the films, a previously published protocol that was applied to $(PLL/HA)_i$ films [38] was again followed. It is based on the reaction of activated carboxylic sites with primary amine groups [39] in the presence of a water-soluble carbodiimide (EDC) and of N-hydroxysulfosuccinimide (sulfo-NHS) (both purchased from Sigma). Briefly, EDC was dissolved at pH 4.5 in the NaCl 0.01M aqueous solution at a final concentration of 100 mg/mL. Sulfo-NHS was dissolved in the same solution at the final constant concentration of 11 mg/mL. The PEI-$(HA/HA^+)_9$-HA and PEI-$(HA/HA^+)_{10}$ coated glass slides were introduced in 24-well culture plates and put in contact with 0.5 mL of the EDC/S mixture during 12 hours at 4°C. Rinsing was performed three times with a 0.01 M NaCl solution for one hour at pH 8 and then the films were rinsed with a 0.15 M NaCl solution at pH 7.4 before being placed in contact with the culture medium.

For film cross-linking characterization, PEI-$(HA/HA^+)_7$-HA films deposited on a ZnSe crystal were investigated by *in situ* Fourier Transform Infrared (FTIR) Spectroscopy in Attenuated Total Reflection (ATR) mode with an Equinox 55 spectrophotometer (Bruker, Wissembourg, France). The experiments were performed in a deuterated 0.01 M NaCl solution at pH 6.5 for the film buildup and pH 4.5 for cross-linking reaction. 4 mL of the mixed EDC/sulfo-NHS solutions were flushed in the measuring cell. The parameters and configuration used for the acquisition during the cross-linking reaction have already been given in detail [38]. Spectra were

acquired before, during, and after cross-linking and were analyzed using the OPUS 2 analysis software (Brucker, Wissembourg, France).

Fibroblasts culture

Fibroblasts NIH3T3 were routinely grown in Dulbecco's Modified Eagle's Medium (DMEM) (GibcoBRL), 10% fetal bovine serum (FBS, Life Technologies), 50 U/mL penicillin, and 50 U/mL streptomycin (Bio-Whittaker) in a 5% CO_2 and 95% air atmosphere at 37 °C. The cells were detached with 0.04% trypsin/EDTA solution (Gibco BRL, UK) and resuspended in a DMEM medium supplemented with antibiotics. The cells were distributed into 24-well plates containing the film coated glass slides (2.5×10^4 cells per well) in a total volume of 1mL of DMEM supplement. The cells were incubated at 37°C under a 5% CO_2 humidified atmosphere. After 24 hours and 72 hours each well was washed with 1 mL PBS, before adding 1 mL of new medium.

Four different types of films were investigated: PEI-$(HA/HA^+)_9$-HA, PEI-$(HA/HA^+)_{10}$, $(PLL/HA)_{12}$ native and cross-linked (noted ~CL) and compared to bare glass. The $(HA/HA^+)_i$ were prepared in the 0.01M NaCl solution at pH 6.5 and were subsequently cross-linked. The native and CL $(PLL/HA)_{12}$ films were built in a 0.15M NaCl solution at pH 6.5.

Cell viability (trypan-blue test)

After four days of culture, the cells were washed with PBS and detached with 100µL trypsin/EDTA (Gibco BRL, UK) at 37°C during 5 minutes. 100µL of DMEM was added and the suspension was collected. The wells were rinsed one more time and resuspended in 100µL of MEM. 60µL of trypan blue were added to 300µL of cell suspension and the whole mixture was gently agitated. The non-coloured cells (the living ones) were finally counted with a Neubauer cell. The experiment was performed twice (with three wells per film condition in each experiment).

Statistical analysis

Data were analyzed using the one-way ANOVA (one-way analysis of variance) from SigmaStat 2.0 (Jandel corporation, Germany) with significance at $p<0.05$.

Results and discussion

Amine modified hyaluronan

Direct carbodiimide-mediated coupling of amines to the carboxyl group of HA in an aqueous environment, e.g., with 1-ethyl-3-[3-dimethylaminopropyl]carbodiimide (EDC), did not yield the predicted product since the O-acyl isourea that is formed as a reactive intermediate rearranges rapidly to a stable N-acylurea [13,40]. In this study, we describe a new synthesis route to afford substituted HA on carboxyl group (Figure 1). We prepared cationic HA by a modified procedure described earlier by Bulpitt and Aeschlimann [13]. In this approach, active HA esters are formed in DMSO with N-hydroxysulfosuccinimide using the water soluble carbodiimide EDC as coupling agent. Nucleophilic addition to the ester formed from Sulfo-NHS requires presenting the mono-protected di-amine in an unprotonated form in the presence of N-ethyl diisopropylamine. The free amine is obtained after deprotection by trifluoroacetic acid. The targeted degree of modification was 100% in order to change all the free carboxylic groups into primary amines. However, the degree of modification as measured by ^{1}H-Nuclear Magnetic Resonance analysis was found to be of 60–80%. On the RMN curve, the chemical signature of the spacer arm on the spectra of HA^+ could clearly be identified (Supporting information, Figure 1). The global charge of the amine modified hyaluronan (HA^+) was then determined by zeta potential. The zeta potential of HA^+ in NaCl 0.01 M at pH 6.5 was found

to be 3.5±0.4 mV. The molecule is thus weakly positively charged. As the amine group can not be clearly identified by FTIR due to the presence of strong alcohol peaks, the amide bond formation resulting from the reaction between amine groups and carboxyl groups of HA was checked. In the IR spectrum of HA^+, the carbonyl absorption band of the carboxylate sodium salt in HA (1606 cm^{-1} and 1406 cm^{-1}) become weaker and the new amide bond appears at 1650 cm^{-1} (Supporting information, Figure 2). These results suggest that the amide bonds between carboxylic groups of HA and amine of NH_2-Peg_2-NH_2 have formed in HA^+.

Film characteristics

The film buildup was characterized by different techniques such as quartz crystal microbalance, atomic force microscopy and Fourier Transform Infrared Spectroscopy. Quartz crystal microbalance was used to investigate the type of film growth and to determine film thickness using the Voinova model [41]. Film thickness was also estimated by AFM by imaging a scratched zone of the film (scratch with a needle). The film roughnesses are also summarized in Table 1.

First, we tried to build films in a physiological ionic strength medium at 0.15M NaCl, as many other polyelectrolyte multilayer films grow in these conditions [20,42 28,43]. For instance, the thickness of (HA/PLL) and (HA/PAH) films is known to be of the order of several hundreds of nanometers after the deposition of only few layer pairs as film growth is of exponential type [28,44]. It is generally observed that films built at higher ionic strength are thicker than those built at low ionic strength [42,45]. This is attributed to the conformation of the polyelectrolytes: at low ionic strength, the polyelectrolyte chains are elongated as the charges are repulsing one another. The polyelectrolyte adsorption leads to a small thickness increase or even to the desorption of polyelectrolyte complexes due to the affinity between opposite charges. At higher ionic strength, the charges are screened and the polyelectrolytes have a random coil shape. The adsorption of these coils lead to a larger thickness increase after each adsorption step. However, the (HA/HA^+) film did not grow in a medium containing 0.15M NaCl (data not shown). Another trial was performed by replacing the polyanion (HA) by a more charged polyanion like PGA (zeta potential of HA is of −50mV for HA [28] and −60 mV for PGA[43] in multilayer films with PLL as polycation), but there was no film growth either (data not shown). As HA^+ is only weakly positively charged, we believe that the growth of HA/HA^+ and PGA/HA^+ films in a salt containing medium (0.15M NaCl) is hampered by the weakness of the interactions between the polyelectrolytes.

As it was recently shown that films containing HA as polyanion and collagen as polycationic biopolymer could be built at low ionic strength (0.01M NaCl) [33,34] where the polymers have a fully extended conformation [46], we investigated the film buildup under low ionic strength conditions for the amine modified hyaluronan. In order to compare (HA/HA^+) film growth with other systems, we analyzed the buildup of various systems under the same experimental conditions (Figure 2). The raw QCM signal obtained for (HA/HA^+) films is plotted as a function of the number of layer pairs (Figure 2A). The experiments have been performed in duplicate and standard deviations are of the order of 5 to 20% (supporting information, Figure 3). However, for more clarity, only one QCM experiment is represented for each type of film. On Figure 2, polycation layers are represented by open symbols and polyanion layers by closed symbols. (HA/HA^+) films are compared to (HA/PLL) and (HA/PAH) films at the same ionic strength, PLL and PAH being more charged polyelectrolytes of shorter chains [47,48]. Film growth is faster for (HA/PAH) films than for (HA/PLL) films, which is qualitatively similar to (HA/HA^+) films. Figure 2B represents the raw QCM signals at 15 MHz but with HA^+ as polycation and PGA and HA as polyanions. In all cases, film growth can be characterized by a linear increase of the thickness as a function of the number of layer pairs when analyzed over the initial ten layer pairs.

We noticed a decrease in frequency shift for (HA/PLL) and for (HA/PAH) films after deposition of the polycation layer (PAH and PLL, open symbols, Figure 2A) and for (PGA/HA^+) after the deposition of the polyanion layer (closed symbols, Figure 2B) is similar to what was observed for (CHI/HA) films at very low ionic strength (10^{-4}M) [30] and for other polyelectrolyte systems [49]. In these previous studies, this observation was attributed to redissolution of the polyelectrolyte complexes following the contact between the film and the polyelectrolyte solution [30,49]. It may also originate from a film swelling or deswelling upon polyelectrolyte adsorption as the dissipation factor was always increasing upon adsorption of the polycation layer for (HA/PLL), (HA/PAH) and (PGA/HA^+) films (data not shown). Similar density changes (film swelling/shrinking) have been observed for (PLL/HA) films built in 0.15M NaCl and are probably due to the modification of the hydration core surrounding hyaluronan upon interaction with the oppositely charged polycation. Water distribution was recently investigated in multilayer films of weak synthetic polyelectrolytes [50] but is still largely unknown in multilayers of weak and highly hydrated polyelectrolytes such as those made of hyaluronan.

This type of curve with successive increases and decreases in frequency upon polyelectrolyte adsorption is not observed for (HA/HA^+) films.

The thicknesses deduced from the four measured frequencies (only the 15MHz curve is represented in Figure 2 for more clarity) and from the viscous dissipation curves (data not shown) are represented in Figure 3. They agree qualitatively with the raw data of Figure 2. A linear increase of the film thicknesses is observed. The measured thickness for films made of ten layer pairs are gathered in Table 1.

The topography and roughness of the films built with polyanionic HA were observed by AFM (Figure 4). All the films are made of small nodules. (HA/PAH) films are the most grainy ones with the highest surface roughness followed by the (HA/PLL) and by (HA/HA^+) films, which are about 2 nm in roughness (Table 1).

The study of (HA/HA^+) film buildup was completed by analysing film secondary structure using ATR-FTIR in D_2O at pH = 6.5. Carboxylic and saccharide peaks evolutions were more particularly followed (Figure 5). Similarly to what has already been observed for (PLL/HA) films [38] and (CHI/HA) films [51] using the same anionic hyaluronan, three main regions could be distinguished: the characteristic saccharide peaks in the 950–1200 cm^{-1} region (not shown) are representative of the skeletal vibrations and involve the C-O stretching at 1082 cm^{-1}, 1032 cm^{-1} and that at 1159 cm^{-1} [52,53]; the band at 1400–1500 cm^{-1} contains the amide II band from HA, and the peak attributed to $-COO^-$ symmetric stretch (1412 cm^{-1}) of HA [54]; the band in the 1630–1700 cm^{-1} region corresponds to the amide I vibrations of HA [54 53], the peak attributed to $-COO^-$ asymmetric stretch from HA (1606 cm^{-1}) (Figure 5A). By plotting the maximum of the peaks at 1606 cm^{-1} (carboxylic peak) and 1081 cm^{-1} (saccharide peak) as a function of the number of layer pairs (Figure 5B), one can observe that the intensity maxima of these peaks increase linearly with the number of deposited layers, which agrees well with the QCM data.

Stability in physiological medium by cross-linking

As the $(HA/HA^+)_i$ films are built in a low ionic strength medium, it was important to check their stability in a physiological medium containing salt (about 0.15 M NaCl) for subsequent cell adhesion studies. Unfortunately, QCM-D data evidenced that, once the medium was changed to a higher ionic strength medium, the signal drastically decreased (data not shown), which probably indicates that the film was suddenly disrupting and not eroding. This may originate from a change in the three dimensional structure of the film due to the modification of the electrostatic forces. Such stability problems were already encountered for other

polyelectrolyte multilayer films built at low pH or/and low ionic strength and then transferred to a physiological medium at pH 7.4 [55] such as PLL/acid poly(L-glutamic) films or (COLL/HA) films [34]. Similar problems exist for hydrogen bonded films that need to be cross-linked prior to their transfer in neutral pH solutions [56]. Film growth is also known to greatly dependent on ionic strength conditions [57,58] and film deconstruction has already been shown to occur for systems containing a weak polyacid when the ionic strength is increased [59,60].

In order to stabilize (HA/HA^+) films for use in physiological media, one had to find a way to strengthen their structure. This may be achieved by film cross-linking. Several cross-linking strategies have been recently developed to enhance both mechanical and chemical stability of polyelectrolyte multilayer films or capsules, including thermal cross-linking [61], chemical cross-linking by glutaraldehyde [62], mild oxydation and disulfide bond formation [63] and cross-linking using carbodiimides [38]. Cross-linking by means of carbodiimides consists in a simple water based protocol of defined chemistry that can be applied to a wide variety of films following their buildup [38,64 37,56], provided that they possess carboxylic and primary amine groups. Therefore, we applied this protocol to the (HA/HA^+) films and followed cross-linking by FTIR (Figure 6).

Spectra were taken at the end of the film buildup (before contact with the EDC/sulfo-NHS solution) and ten hours after contact with the EDC/sulfo-NHS solution (after cross-linking). They are represented in Figure 6 together with the difference between the actual spectrum and the spectrum recorded before contact with the cross-linker solution. The intensity of the peaks attributed to the carboxylic groups (1606, 1412 cm^{-1}) decreased and correlatively the intensity of the amide bands increased (1620–1680 cm^{-1} and 1400–1500 cm^{-1}). This was a strong indication of the formation of amide bonds between HA^+ and HA at the expense of carboxylic groups. A second, although indirect, proof for the effective cross-linking concerned the invariance of the FTIR spectrum when the film is put in contact with a 0.15 M NaCl solution (data not shown).

Fibroblasts adhesion onto the films

For subsequent cell adhesion studies, it was a prerequisite that the film remained stable in physiological medium. Therefore, only cross-linked (HA/HA^+) films were investigated for cell culture studies. Hyaluronan gels are usually found to be anti-adhesive for cells unless surface modification is performed by various strategies such as coating with poly(D-lysine) [65], grafting the adhesive RGD peptide [66] or including gelatin in the gels [67]. With respect to polyelectrolyte multilayer films containing hyaluronan, a poor cell adhesion was always observed on films like (PLL/HA) [38] or (CHI/HA) [30] unless the films were cross-linked. This was attributed to their high water content, their gel like character and their softness [38,68]. We indeed recently found that chondrosarcoma adhesion and spreading depended on the extent of film cross-linking [69]. Micropatterned cell co-cultures were also recently achieved with the layer-by-layer technique using hyaluronan as non adhesive substrate and poly(L-lysine) [70] or COLL as adhesive substrates [29]. Here, we compared the (HA/HA^+) films terminating by either HA or HA^+ to the already well characterized (PLL/HA) native and cross-linked films [38]. The viability of NIH3T3 cells was evaluated after four days in culture. The number of living cells on cross-linked (HA/HA^+) films was slightly lower than that on cross-linked (PLL/HA) films, cell number being slightly higher on films ending by HA. This proved the good biocompatibility of pure hyaluronan films. For (PLL/HA) films, the change in cell adhesion upon cross-linking was attributed mainly to a change in film stiffness [71]. One may hypothesize that cross-linking also leads to a change in (HA/HA^+) film mechanical properties. Unfortunately, these properties can not be measured directly by AFM colloidal probe due to the small sample thickness (about 100 nm).

Such (HA/HA^+) thin films are potentially interesting for biomedical applications as they allow the deposition of hyaluronan layers with a nanometer scale control. They could be employed for fundamental cell adhesion studies aimed at understanding the mechanism of cell/substrate interactions [6]. In addition, as hyaluronan can be grafted with various types of molecules ([72, 73 74]), the films may be functionalized by adsorption of a bioactive layer as last deposited layer. They may also be functionalized by direct diffusion of drugs into the film after its cross-linking, as was recently shown on cross-linked PEM films (Schneider, in press, [75]).

CONCLUSION

Biochemical surface functionalization is important for a wide range of bioengineering applications. In particular, adsorption or grafting of molecules such as biopolymers, proteins or polysaccharides has gained lots of attention and many studies focus on the characterization of modified surfaces for cell culture studies. Hyaluronan enters in this category and is widely investigated for its biological and physico-chemical properties. Here, the formation of a new kind of thin films based on hyaluronan and chemically modified hyaluronic acid was investigated. The layer-by-layer technique was employed to prepare thin films of hyaluronan of tunable thickness at the nanometer scale. These films were stable in physiological media once cross-linked by means of carbodiimide chemistry such as to form covalent amide bonds between amino groups of modified hyaluronic acid and carboxylic groups of hyaluronan. NIH 3T3 cells were viable onto thin films of hyaluronan with however better results for hyaluronan ending films. These films may now constitute the basis for more quantitative cell adhesion studies using biophysical techniques. They could also constitute a platform for the introduction of bioactive molecules within the film architecture in order to get biofunctionalized material surfaces.

Supplementary Material

Refer to Web version on PubMed Central for supplementary material.

ACKNOWLEDGMENTS

This work has been partly supported by the Action Concertée Incitative "Nanosciences" (ACI NR204) from the Ministère Français de la Recherche, by the NIH via a subcontract to CP (R21, n°544168A) and by the “Association Recherche sur le Cancer” (ARC, grant n° 7916 to CP). AS is indebted to the « Region Alsace » for financial support.

REFERENCES

1. Laurent, TC. The chemistry, biology, and medical applications of hyaluronan and its derivatives. Vol. 72. Cambridge, U.K.: Cambridge University Press; 1998.
2. Peattie RA, Rieke ER, Hewett EM, Fisher RJ, Shu XZ, Prestwich GD. Biomaterials 2006;27:1868–1875. [PubMed: 16246413]
3. Morra M. Biomacromolecules 2005;6:1205–1223. [PubMed: 15877335]
4. Weindl G, Schaller M, Schafer-Korting M, Korting HC. Skin Pharmacology and Physiology 2004;17:207–213. [PubMed: 15452406]
5. Zimmerman E, Geiger B, Addadi L. Biophys. J 2002;82:1848–1857. [PubMed: 11916844]
6. Cohen M, Kam Z, Addadi L, Geiger B. Embo Journal 2006;25:302–311. [PubMed: 16407968]
7. Cattaruzza S, Perris R. Matrix Biology 2005;24:400–417. [PubMed: 16055321]
8. Prestwich GD, Marecak DM, Marecek JF, Vercruysse KP, Ziebell MR. J Control Release 1998;53:93–103. [PubMed: 9741917]
9. Nettles DL, Vail TP, Morgan MT, Grinstaff MW, Setton LA. Ann. Biomed. Eng 2004;32:391–397. [PubMed: 15095813]

10. Segura T, Anderson BC, Chung PH, Webber RE, Shull KR, Shea LD. Biomaterials 2005;26:359–371. [PubMed: 15275810]
11. Crescenzi V, Francescangeli A, Taglienti A. Biomacromolecules 2002;3:1384–1391. [PubMed: 12425680]
12. Arimura H, Ouchi T, Kishida A, Ohya Y. J. Biomater. Sci. Polym. Ed 2005;16:1347–1358. [PubMed: 16370238]
13. Bulpitt P, Aeschlimann D. J. Biomed. Mater. Res 1999;47:152–169. [PubMed: 10449626]
14. Smeds KA, Pfister-Serres A, Miki D, Dastgheib K, Inoue M, Hatchell DL, Grinstaff MW. J Biomed Mater Res 2001;54:115–121. [PubMed: 11077410]
15. Baier Leach J, Bivens KA, Patrick CW Jr, Schmidt CE. Biotechnol. Bioeng 2003;82:578–589. [PubMed: 12652481]
16. Luo Y, Kirker KR, Prestwich GD. J. Control. Release 2000;69:169–184. [PubMed: 11018555]
17. Luo Y, Prestwich GD. Curr Cancer Drug Targets 2002;2:209–226. [PubMed: 12188908]
18. Suh KY, Yang JM, Khademhosseini A, Berry D, Tran TN, Park H, Langer R. J Biomed Mater Res B Appl Biomater 2005;72:292–298. [PubMed: 15486967]
19. Mason M, Vercruysse KP, Kirker KR, Frisch R, Marecak DM, Prestwich GD, Pitt WG. Biomaterials 2000;21:31–36. [PubMed: 10619676]
20. Decher G, Hong JD, Schmitt J. Thin Solid Films 1992;210–211:831–835.
21. Decher G, Lehr B, Lowack K, Lvov Y, Schmitt J. Biosens. Bioelectron 1994;9:677–684.
22. Decher G. Science 1997;277:1232–1237.
23. Lvov, YM. Handbook of Surfaces and Interfaces of Materials; Vol 3: Nanostructures Materials, Micelles, and Colloids. Nalwa, HS., editor. Academic Press; 2001.
24. Rmaile HH, Schlenoff JB. J. Am. Chem. Soc 2003;125:6602–6603. [PubMed: 12769548]
25. Serizawa T, Yamaguchi M, Kishida A, Akashi M. Journal of Biomedical Materials Res A 2003;67:1060–1063.
26. Miller MD, Bruening ML. Chem. Mater 2005;17:5375–5381.
27. Ai H, Jones SA, Lvov YM. Cell Biochem. Biophys 2003;39:23–43. [PubMed: 12835527]
28. Picart C, Lavalle P, Hubert P, Cuisinier FJG, Decher G, Schaaf P, Voegel J-C. Langmuir 2001;17:7414–7424.
29. Fukuda J, Khademhosseini A, Yeh J, Eng G, Cheng J, Farokhzad OC, R L. Biomaterials 2006;27:1479–1486. [PubMed: 16242769]
30. Richert L, Lavalle P, Payan E, Stoltz J-F, Shu XZ, Prestwich GD, Schaaf P, Voegel J-C, Picart C. Langmuir 2004;1:284–294.
31. Thierry B, Winnik FM, Merhi Y, Silver J, Tabrizian M. Biomacromolecules 2003;4:1564–1571. [PubMed: 14606881]
32. Burke SE, Barrett CJ. Biomacromolecules 2005;6:1419–1428. [PubMed: 15877361]
33. Zhang J, Senger B, Vautier D, Picart C, Schaaf P, Voegel J-C, Lavalle P. Biomaterials 2005;26:3353–3361. [PubMed: 15603831]
34. Johansson JA, Halthur T, Herranen M, Soderberg L, Elofsson U, Hilborn J. Biomacromolecules 2005;6:1353–1359. [PubMed: 15877352]
35. Hook F, Rodahl M, Brzezinski P, Kasemo B. Journal of Colloid and Interface Science 1998;208:63–67. [PubMed: 9820749]
36. Rodahl M, Kasemo B. Rev. Sci. Instrum 1996;67:3238–3241.
37. Picart C, Elkaim R, Richert L, Audoin F, Da Silva Cardoso M, Schaaf P, Voegel J-C, Frisch B. Adv. Funct. Mater 2005;15:83–94.
38. Richert L, Boulmedais F, Lavalle P, Mutterer J, Ferreux E, Decher G, Schaaf P, Voegel J-C, Picart C. Biomacromolecules 2004;5:284–294. [PubMed: 15002986]
39. Hermanson, GT. Bioconjugate techniques. Academic Press; 1996. p. 169-176.
40. Luo Y, Prestwich GD. Bioconjugate Chem 2001;12:1085–1088.
41. Voinova MV, Rodahl M, Jonson M, Kasemo B. Physica Scripta 1999;59:391–396.
42. Ladam G, Schaad P, Voegel J-C, Schaaf P, Decher G, Cuisinier FJG. Langmuir 2000;16:1249–1255.

43. Lavalle P, Gergely C, Cuisinier F, Decher G, Schaaf P, Voegel J-C, Picart C. Macromolecules 2002;35:4458–4465.
44. Ball V, Hubsch E, Schweiss R, Voegel JC, Schaaf P, Knoll W. Langmuir 2005;21:8526–8531. [PubMed: 16114967]
45. Tjipto E, Quinn JF, Caruso F. Langmuir 2005;21:8785–8792. [PubMed: 16142961]
46. Barrat J, Joanny JF. Advances in Chemical Physics 1996;XCIV:1–66.
47. Cong R, Temyanko E, Russo P, Edwin N, Uppu R. Macromolecules 2006;39:731–739.
48. Forster S, Schmidt M, Antonietti M. J. Phys. Chem 1992;96:4008–4014.
49. Kovacevic D, van der Burgh S, de Keizer A, Cohen Stuart MA. Langmuir 2002;18:5607–5612.
50. Tanchak OM, Yager KG, Fritzsche H, Harroun T, Katsaras J, Barrett CJ. Langmuir 2006;22:5137–5143. [PubMed: 16700605]
51. Picart C, Schneider A, Etienne O, Mutterer J, Egles C, Jessel N, Voegel J-C. Adv. Funct. Mater 2005;15:1771–1780.
52. Wang XH, Li DP, Wang WJ, Feng QL, Cui FZ, Xu YX, Song XH, van der Werf M. Biomaterials 2003;24:3213–3220. [PubMed: 12763448]
53. Duarte ML, Ferreira MC, Marvao MR, Rocha J. Int. J. Biol. Macromol 2002;31:1–8. [PubMed: 12559421]
54. Haxaire K, Marechal Y, Milas M, Rinaudo M. Biopolymers 2003;72:10–20. [PubMed: 12400087]
55. Richert L, Arntz Y, Schaaf P, Voegel J-C, Picart C. Surf. Sci 2004;570:13–29.
56. Kozlovskaya V, Kharlampieva E, Mansfield M, Sukhishvili S. Chem. Mater 2006;18:328–336.
57. Hoogeveen NG, Cohen Stuart MA, Fleer GJ, Böhmer MR. Langmuir 1996;12:3675–3681.
58. Schoeler B, Kumaraswamy G, Caruso F. Macromolecules 2002;35:889–897.
59. Schüler C, Caruso F. Biomacromolecules 2001;2:921–926. [PubMed: 11710050]
60. Dubas ST, Schlenoff JB. Macromolecules 2001;34:3736.
61. Harris JJ, DeRose P, Bruening M. J. Am. Chem. Soc 1999;121:1978–1979.
62. Leporatti S, Voigt A, Mitlöhner R, Sukhorukov G, Donath E, Möhwald H. Langmuir 2000;16:4059–4063.
63. Li B, Haynie DT. Biomacromolecules 2004;5:1667–1670. [PubMed: 15360273]
64. Schuetz P, Caruso F. Adv. Funct. Mater 2003;13:929–937.
65. Liu Y, Zheng Shu X, Prestwich GD. Biomaterials 2005;26:4737–4746. [PubMed: 15763253]
66. Shu XZ, Ghosh K, Liu Y, Palumbo FS, Luo Y, Clark RA, Prestwich GD. J. Biomed. Mater. Res 2004;68A:365–375.
67. Shu XZ, Liu Y, Palumbo F, Prestwich GD. Biomaterials 2003;24:3825–3834. [PubMed: 12818555]
68. Richert L, Schneider A, Vautier D, Jessel N, Payan E, Schaaf P, Voegel J-C, Picart C. Cell Biochem. Biophys 2006;44:273–276. [PubMed: 16456228]
69. Schneider A, Francius G, Obeid R, Schwinté P, Frisch B, Schaaf P, Voegel J-C, Senger B, Picart C. Langmuir 2006;22:1193–1200. [PubMed: 16430283]
70. Khademhosseini A, Suh KY, Yang JM, Eng G, Yeh J, Levenberg S, Langer R. Biomaterials 2004;25:3583–3592. [PubMed: 15020132]
71. Richert L, Engler AJ, Discher DE, Picart C. Biomacromolecules 2004;5:1908–1916. [PubMed: 15360305]
72. Luo Y, Ziebell MR, Prestwich GD. Biomacromolecules 2000;1:208–218. [PubMed: 11710102]
73. Thierry B, Kujawa P, Tkaczyk C, Winnik FM, Bilodeau L, Tabrizian M. J. Am. Chem. Soc 2005;127:1626–1627. [PubMed: 15700982]
74. Charlot A, Heyraud A, Guenot P, Rinaudo M, Auzely-Velty R. Biomacromolecules 2006;7:907–913. [PubMed: 16529430]
75. Schneider A, Vodouhê A, Richert L, Francius G, Le Guen E, Schaaf P, Voegel J-C, Frisch F, Picart C. Biomacromolecules. in press

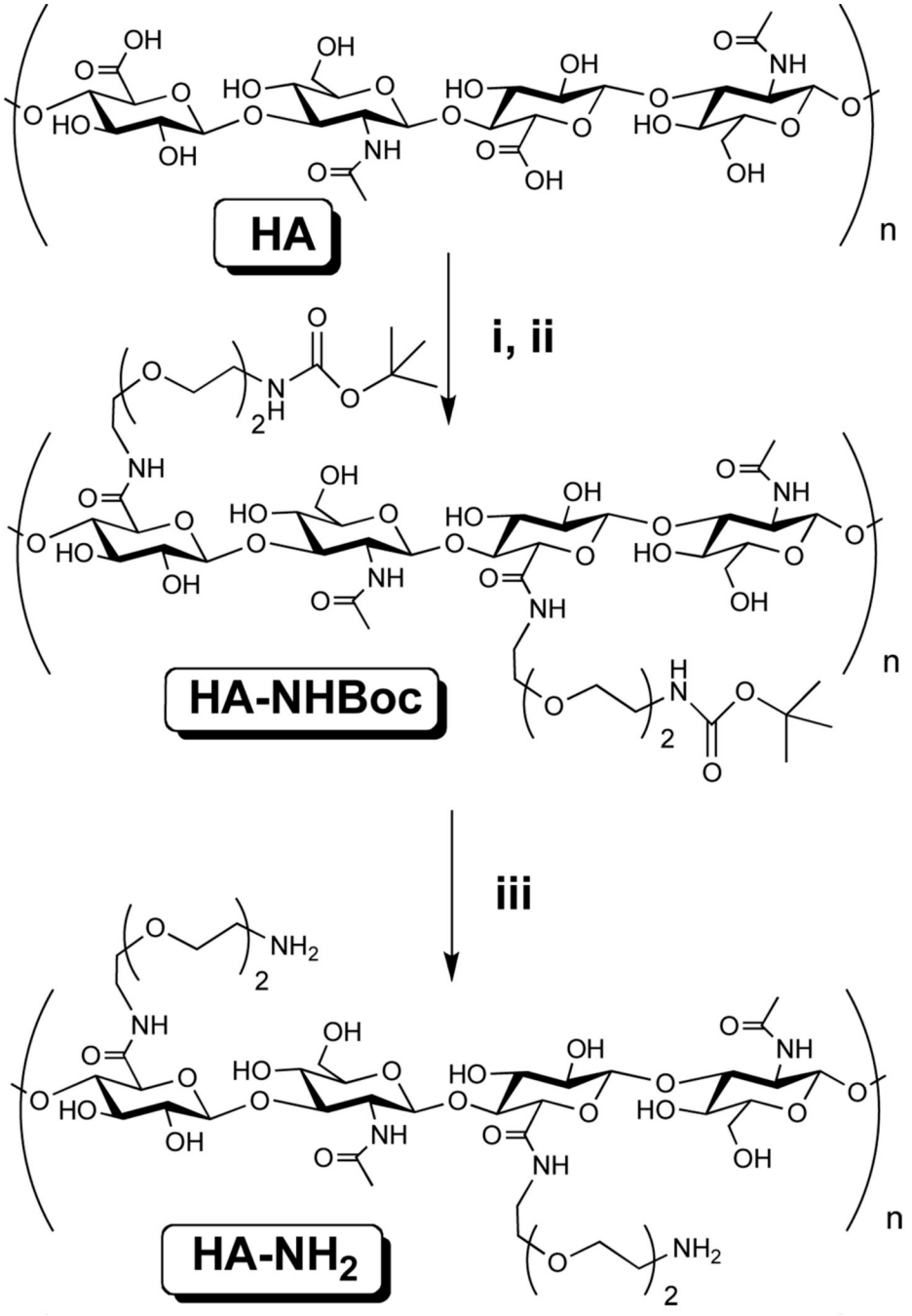

FIGURE 1.

Synthesis of the amine modified hyaluronan. Step i) HA was dissolved in DMSO in the presence of sulfo-NHS and EDC ii) Protection of the HA by the amine NH_2PEG_2NHBoc in the presence of N-ethyl diisopropylamine iii) deprotection of the amine group by dissolution in TFA.

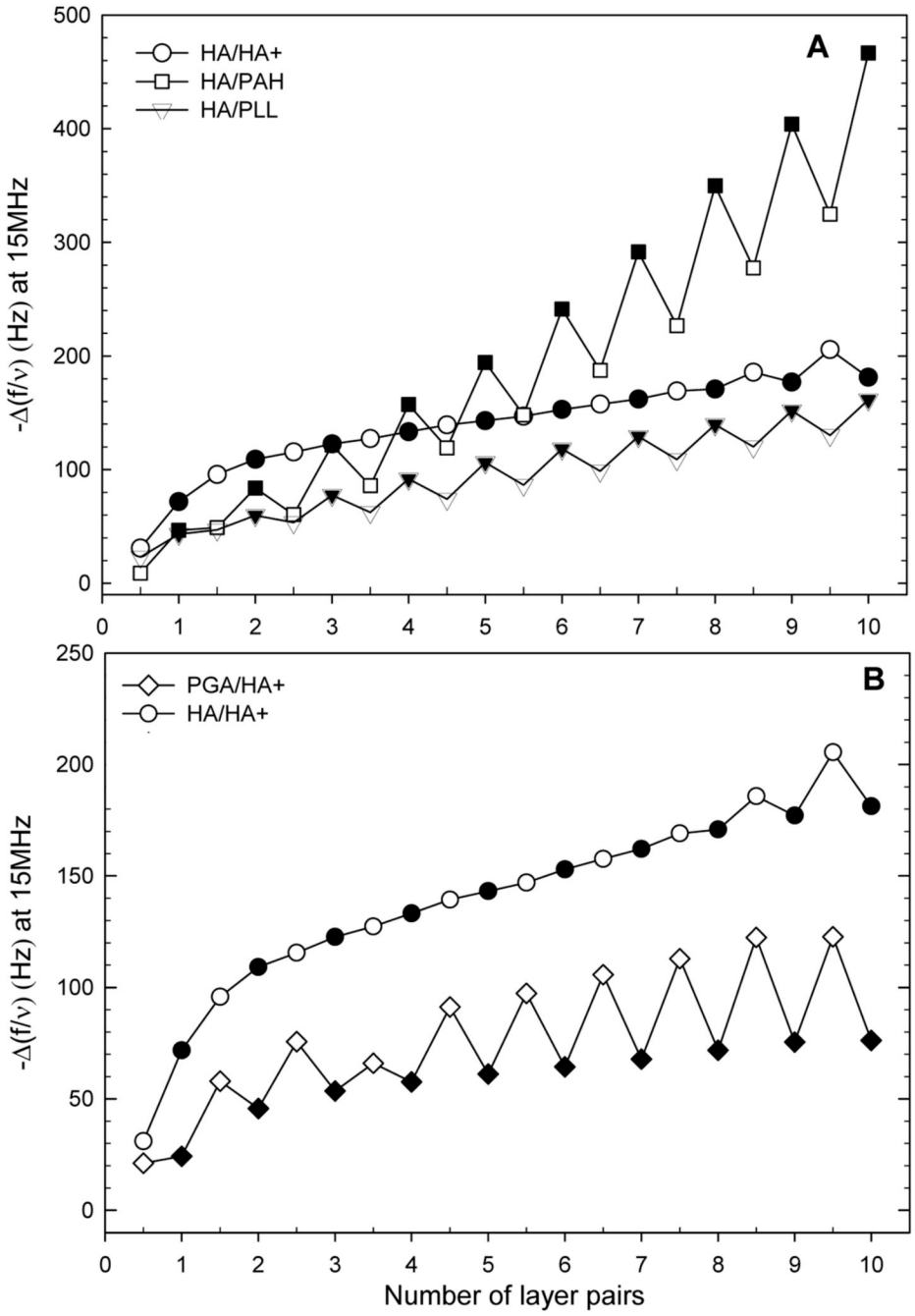

FIGURE 2.

Film growth in 0.01M NaCl (pH 6.5) for different polyelectrolyte multilayer films as measured by QCM-D. Differences in the QCM frequency shifts −Δf/ν measured at 15 MHz at the end of each polycation (open symbols) and polyanion (closed symbols) deposition, after the rinsing step. (A) with HA as polyanions: (HA/HA^+)(○/●), (HA/PAH) (□/■) and (HA/PLL) (▽/▼); (B) with HA^+ as polycation: (HA/HA^+) (○/●) and (PGA/HA^+) and (♦/◊).

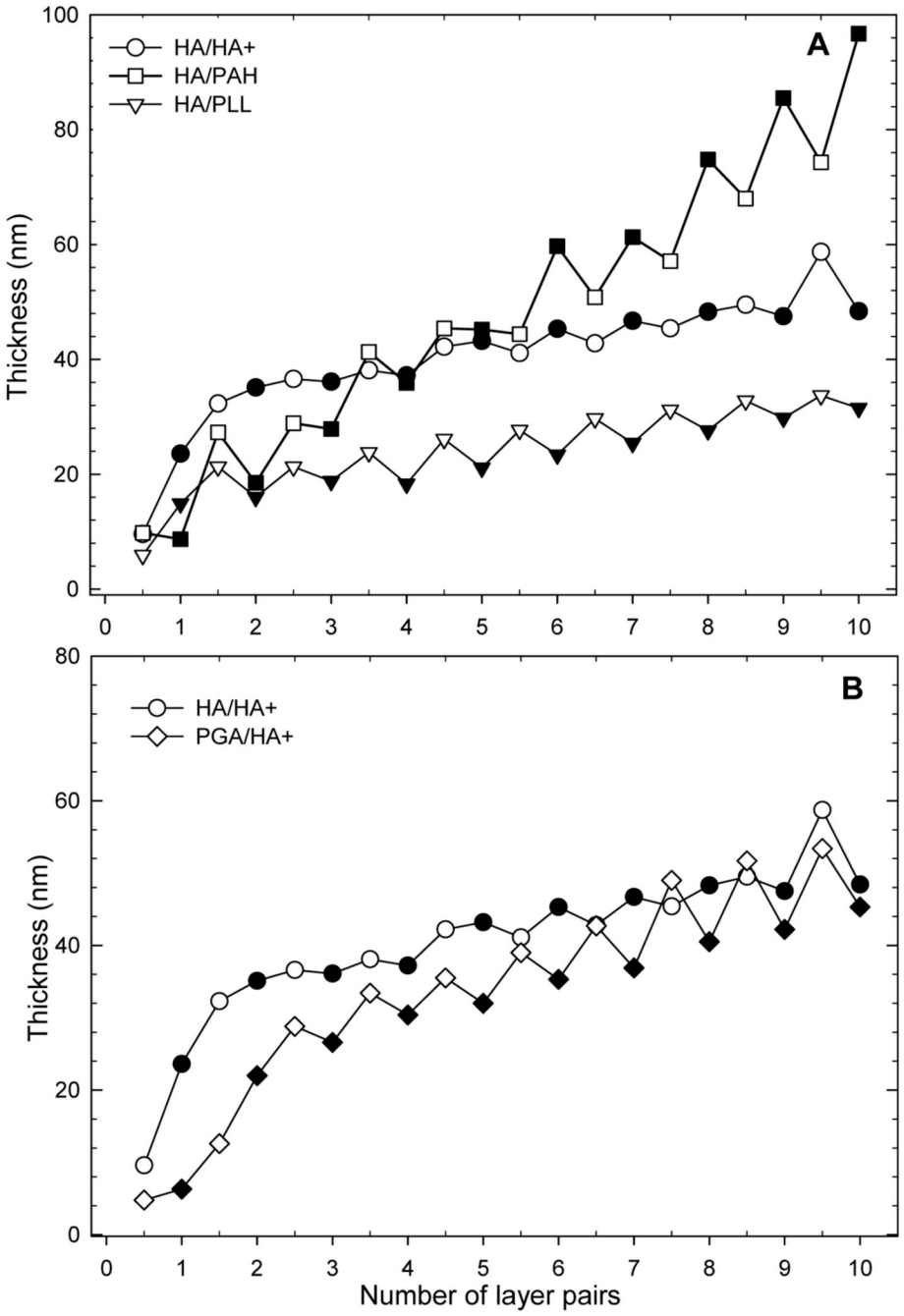

FIGURE 3.

Film thicknesses as a function of the number of layer pairs as estimated by QCM-D (same experimental conditions as in Figure 2). Polycations are represented by open symbols and polyanions by closed symbols for different types of films. (A) with HA as polyanion: (HA/HA^+) (○/●), (HA/PAH) (□/■) and (HA/PLL) (▽/▼); (B) with HA^+ as polycation: (HA/HA^+) (○/●) and (PGA/HA^+) and (♦/◊).

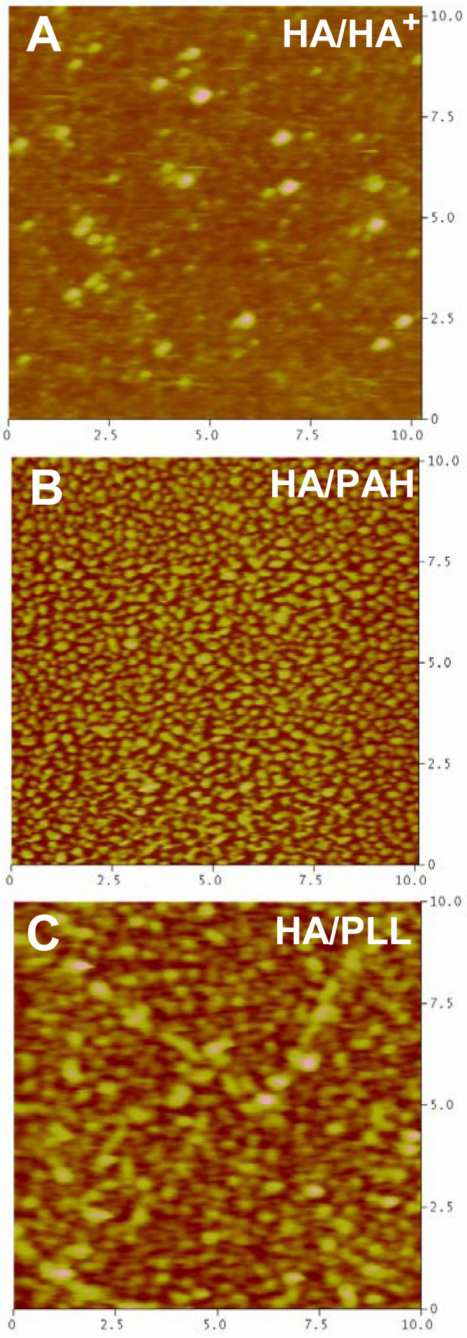

FIGURE 4.

AFM height mode images in liquid obtained for (A) $(HA/HA^{+})_{10}$ (B) $(HA/PAH)_{10}$ and (C) $(HA/PLL)_{10}$. The image dimensions are 10×10 μm^2 and the maximum z-range is 100 nm.

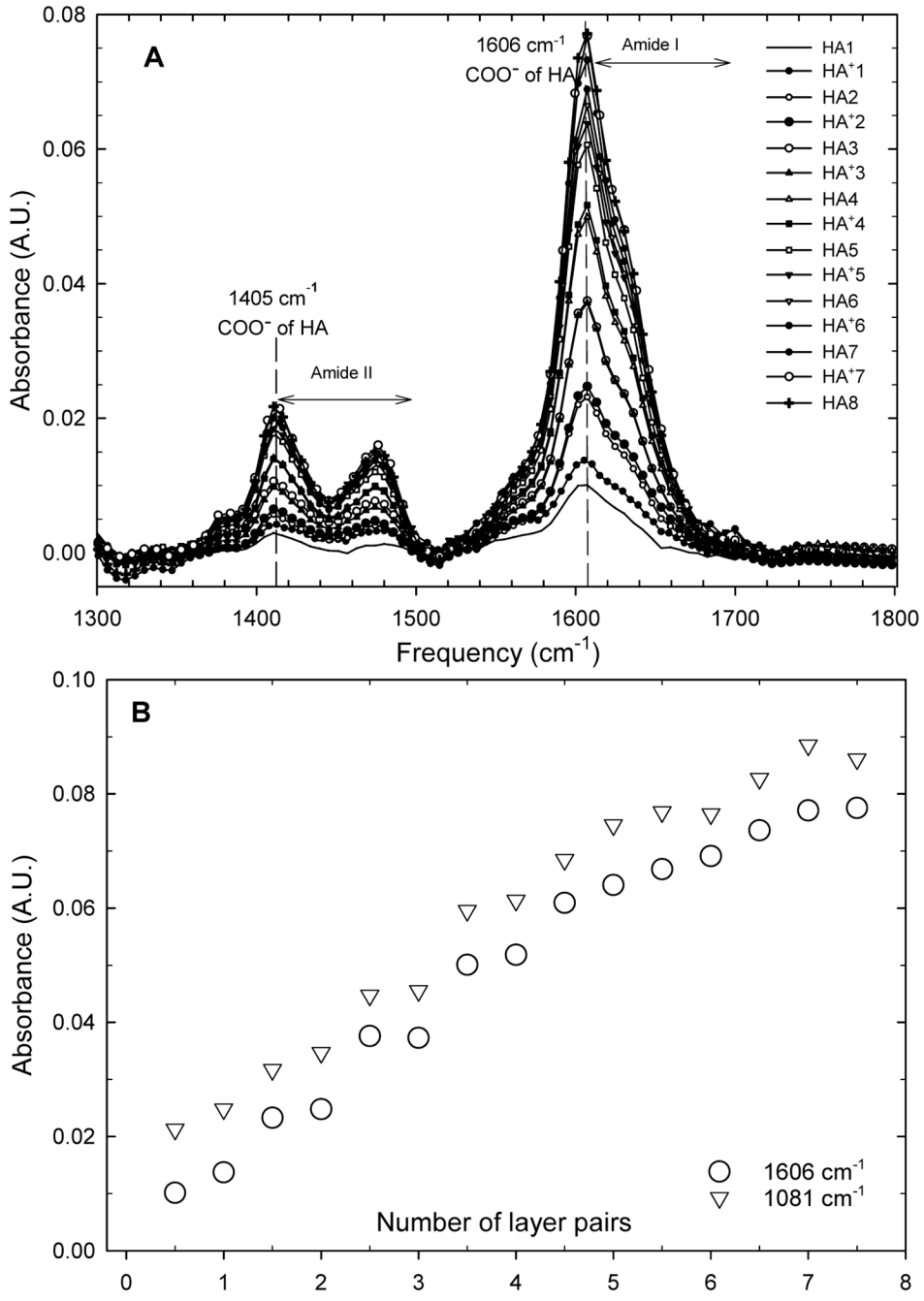

FIGURE 5.

(A) ATR-FTIR spectra of a PEI-$(HA/HA^+)_7$-HA film during its buildup. The spectra are taken after each HA and HA^+ adsorption (after the rinsing step). The carboxylic peaks (1606 and 1412 cm^{-1}, respectively) and the amide I and II bands (1600–1675 and 1400–1500 cm^{-1}, respectively) can be seen. (B) The evolution of the absolute values of the absorbance at 1606 cm^{-1} (○, carboxylic peak) and 1081 cm^{-1} (▽, saccharide peak) is represented as a function of the number of deposited layer pairs.

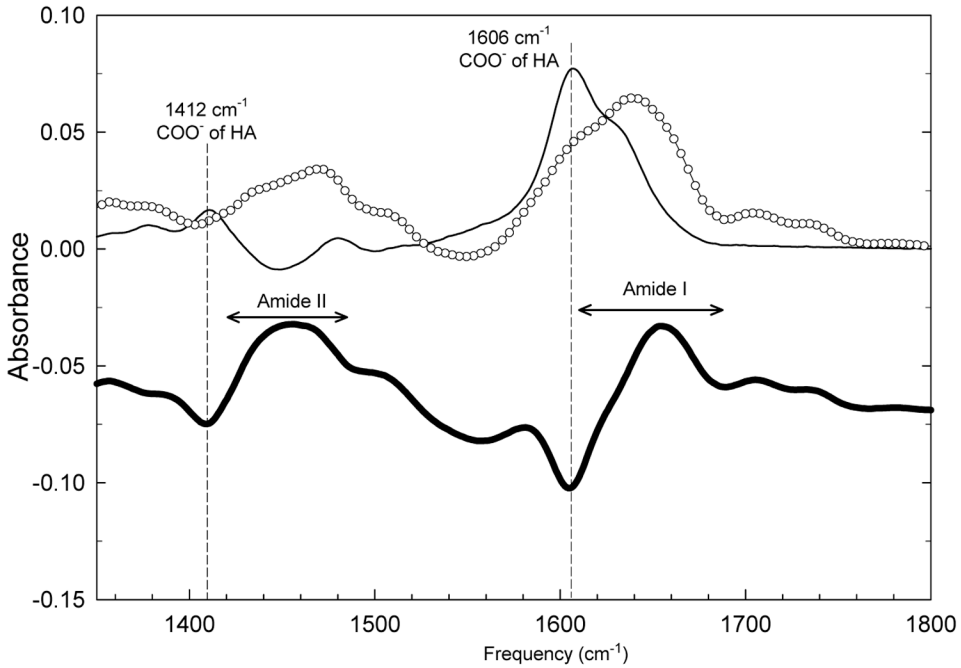

FIGURE 6.

ATR-FTIR spectra of native and cross-linked PEI-$(HA/HA^{+})_7$-HA films before (—) and after cross-linking and final rinsing step (–○–). Cross-linking was achieved by contact with EDC/NHS solution for 12 hours at 4°C. The difference between the two spectra (before and after cross-linking) is also represented (thick black line).

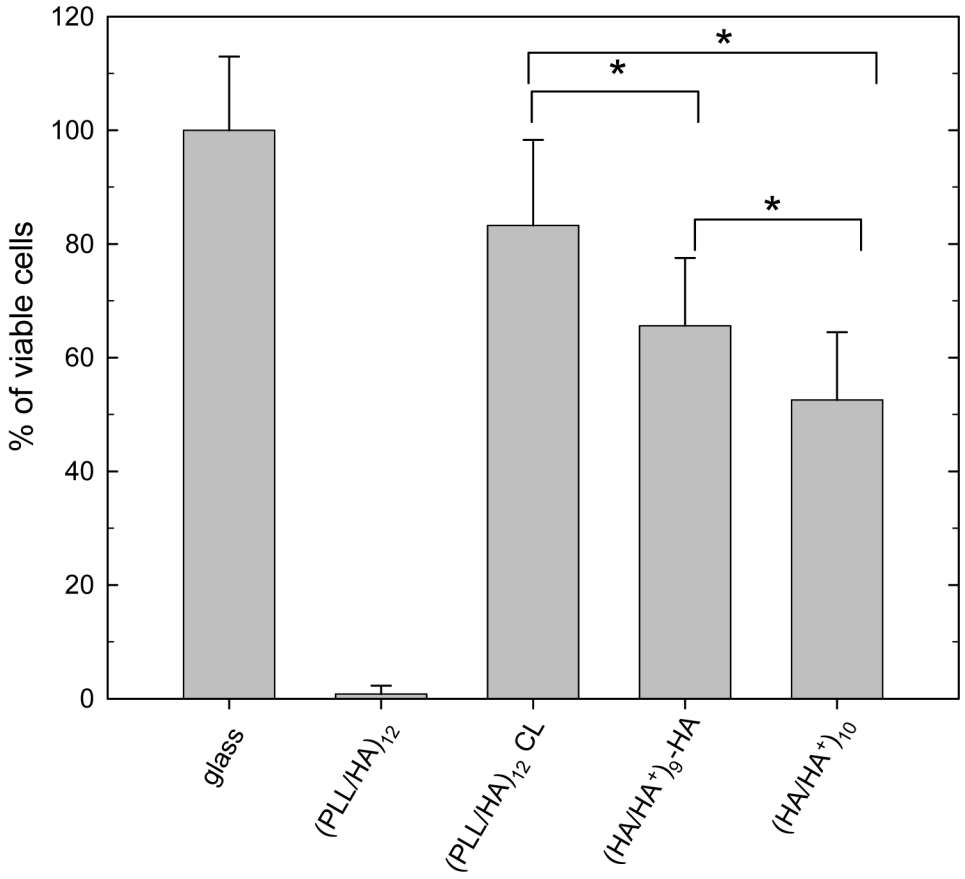

FIGURE 7.

Results of trypan blue test (cell viability) for NIH3T3 cells cultured on different types of films for four days: PEI-$(HA/HA^+)_9$-HA, PEI-$(HA/HA^+)_{10}$, as compared to $(PLL/HA)_{12}$ native or cross-linked films and to bare glass. Values and standard errors are obtained for three slides per film type. *Adhesion was statistically different between different film types (ANOVA, $*p < 0.05$).

Table 1

Summary of the $(HA/HA)^+$ films characteristics and comparison to different polyelectrolyte multilayer films containing either HA^+ as polycation $(PGA/HA)^+$ or HA as polyanion ((HA/PLL) and (HA/PAH)). Films were composed of ten layer pairs. The type of growth was estimated by Quartz Crystal Microbalance (QCM-D).

HA^+ as polycation	**Thickness (nm)**	**0.01M Roughness (nm)**	**Type of growth**	**Thickness (nm)**	**0.15M Roughness (nm)**	**Type of growth**
HA/HA^+	58.7[a]	2.1 ± 0.3[b]	linear	----	No buildup	----
PGA/HA^+	45.3[a]	3.9 ± 0.9[b]	linear	----	No buildup	----
HA as polyanion		**0.01M**			**0.15M**	
HA/PAH	96.7 [a]	5.2 ± 0.1[b]	linear	NA	≈ 545 nm	exponential
HA/PLL	31.5 [a]	4.9 ± 0.1[b]	linear	NA	≈ 900 nm	exponential

[a] Thicknesses were measured by QCM-D

[b] roughnesses were measured by AFM.